Raman Spectral Studies of Aqueous Zinc Nitrate Solution at High Temperatures and at a High Pressure of 30 MPa

Yutaka Ikushima,*,† Norio Saito,† and Masahiko Arai‡

National Industrial Research Institute of Tohoku, Nigatake, Miyagino-ku, Sendai 983-8551, Japan, and Institute for Chemical Reaction Science, Tohoku University, Katahira, Aoba-ku, Sendai 980-8577, Japan

Received: December 8, 1997; In Final Form: February 10, 1998

We present the first direct measurement of dynamic behavior of ions in an aqueous solution at high temperatures and pressure using Raman spectroscopy. We have studied the N−O symmetric stretching mode at high temperatures up to 340 °C and at a high pressure of 30 MPa. The Raman spectra of 1.3 M aqueous zinc nitrate solution have been analyzed by curve fitting. The zinc ion forms two species. In one species Zn^{2+} is bound more strongly to the NO_3^-, and in the other Zn^{2+} is bound more strongly to H_2O. The ratio of the former to the latter remains unaltered with temperatures below 300 °C, but above 300 °C the ratio increases significantly. The average number of water molecules bound to Zn^{2+} (n_{H_2O}) is estimated using the intensity of peak frequency of the symmetric stretching mode of the haxaaquazinc(II) cation. As the temperature increases, the n_{H_2O} gradually decreases, but above 300 °C it shows a large decrease, suggesting the displacement of water molecules from the first solvation shell around Zn^{2+} and the concomitant entry of NO_3^- into the shell. The perpendicular orientational relaxation time ($\tau_\perp$) decreases significantly with temperature; the values of $\tau_\perp$ were 1.86 and 0.25 ps, respectively, at 20 and 340 °C. The Arrhenius plot gives two activation energies, 2.1 kcal mol^{-1} below 300 °C and 6.4 kcal mol^{-1} above 300 °C. The activation energy for the orientational motion, 6.4 kcal mol^{-1}, is larger than that for orientational motion of water, 4−5 kcal mol^{-1}, and we assume that orientational motion of the anion above 300 °C requires the breaking of water−water hydrogen bonds. Furthermore, the experimental values of the perpendicular diffusion constant ($D_\perp$) at higher temperatures than 300 °C are in agreement with those of D_i calculated from the slightly damped free-rotor (SDFR) model, and the rotation around the C_3 axis of the anion is confirmed to proceed rapidly and approach that in the free dilute gas phase.

Introduction

Studies of aqueous electrolyte solutions at high temperatures and pressures are important in not only geochemistry but, more recently, hazardous waste destruction.[1−5] The macroscopic properties of water and electrolyte solutions have been studied in hydrothermal aqueous environments, and thermodynamic properties are known to change widely with pressure and temperature;[6,7] for example, the static dielectric constant of water, ϵ, is about 80 for the liquid water and it decreases to about 3−20 [8] in the supercritical region. This aspect has significant influence on ion−ion and ion−water interactions. One would expect an increase in the attractive forces between cations and anions due to a significant decrease in the ϵ value at high temperatures. However, we have not sufficiently understood the structure of salts in water at the molecular level at high temperatures and pressures to make such predictions. This hinders the development of new technological concepts in disciplines of chemical reactions and separations for hazardous waste destruction and other practical processes.

Several experimental results concerning the ion−solvent interaction at ambient temperature have been provided by neutron scattering[9,10] and Raman spectroscopy.[11−14] In recent years, in addition to Monte Carlo[15,16] and molecular dynamics simulations,[17−19] ion solvation in subcritical and supercritical water has been studied by in situ spectroscopies.[20−27] For instance, XAFS results[22] for Rb^+ in supercritical water solution show that there is a well-defined hydration shell around the cation even at 424 °C but the extent of hydration is significantly reduced. The ion associations in aqueous zinc, cadmium, and calcium nitrate solutions have been studied by Raman spectroscopy.[25,26] The divalent cations produce two species and pass from the solvent-separated cation−anion pairs at lower temperatures into the neighboring cation−anion pairs such as the monovalent cations at higher temperatures. Although these results give information regarding the structure of water around the ion, one cannot understand any participation of solvated ion in the "*time domain*" at all. In order to comprehend the "*true*" mechanisms of ion−ion and ion−water interactions and the temporary structures of the electrolyte solution at high temperatures and pressures, it is necessary to obtain direct information on ion behavior including the rotational relaxation in such a severe environment.

Although Raman spectroscopic studies have been carried out extensively on metal nitrate solutions[28] under ambient conditions, the Raman data have been scarcely presented at high temperatures and pressures.[24,25] For example, our knowledge of the temperature dependence of the rotational dynamics below 100 °C has been developed to a considerable extent;[13,29] however, that of the rotational dynamics of ions at higher

* To whom correspondence should be addressed. E-mail: ikushima@tniri.go.jp.
† National Industrial Research Institute of Tohoku.
‡ Tohoku University. E-mail:marai@icrs.tohoku.ac.jp.

S1089-5647(98)00458-1 CCC: $15.00
Published on Web 03/26/1998

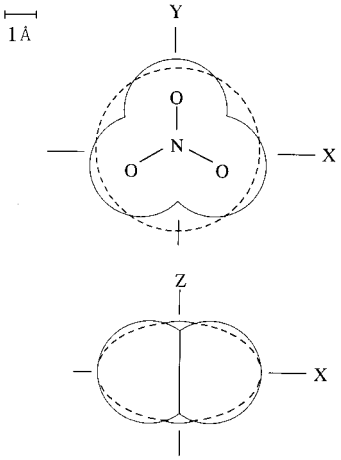

Figure 1. Size and shape of the nitrate ion. *Z* axis corresponds to the C_3 axis of the nitrate ion with D_{3h} symmetry. The nitrate ion is approximately expressed by the spheroid indicated by the broken lines. The long and short axes are 2.6 and 1.5 Å long, respectively.

temperatures and high pressures is lacking. Hence, little has been known about ion−ion and ion−water interactions, microstructures of ion hydration, and diffusional motion of salts on the molecular level in water in the high-temperature and high-pressure region.

We have recently succeeded in the development of a high-temperature and high-pressure Raman spectroscopic system,[30,31] and further improvements in Raman techniques for a hydrothermal aqueous environment as well as the introduction of useful theoretical models make it now possible to understand dynamical properties of aqueous electrolyte solutions in addition to local molecular structures around ions under severe conditions, that is, in supercritical and subcritical water. So we have embarked on the study of the rotational diffusional motion of polyatomic ions and the ion hydration in water at high temperatures and pressures by using the developed system and Raman line-shape analysis.[32]

In the present work, we report Raman data of aqueous nitrate solution of Zn^{2+} up to 360 °C and 30 MPa with a fixed, not concentrated, salt concentration (1.3 M). We discuss ion-hydration behavior in the local environment in the zinc nitrate solution using a simple model.[24] Furthermore, we first present the temperature dependence of the orientational dynamics of the nitrate ion with D_{3h} symmetry in the zinc nitrate solution, for which we analyze the isotropic and anisotropic Raman line shape of the totally symmetric N−O stretching fundamental (ν_1) near 1050 cm^{-1} by a VV−VH (V is vertical, H is horizontal) polarization experiment. In the case of nitrate ion, when the depolarized spectrum of the ν_1 mode is converted to a product of the reorientational and the vibrational relaxation function by Fourier transformation, the Raman technique leads to the monitor of the rotation around the axes perpendicular to the C_3 axis (*Z* axis in Figure 1), which is called the perpendicular rotation.[11,13,33] On the other hand, the rotation around the C_3 axis, which is called the parallel rotation, can be monitored by the ^{17}O NMR technique.[14] We have reported significant results concerning the mechanism of the anisotropic rotations of the nitrate ion in water at high temperature and pressure.

Experimental and Data Analysis Section

Materials. Zinc nitrate salt of guaranteed reagent grade was purchased from Wako Chemical Co. Inc. Triply distilled high-purity water was used and degassed by N_2 gas prior to use. The zinc nitrate solution was filtered through a Millipore filter to remove dusts contained.

Raman Experiment. The main difficulty in laser Raman spectroscopic investigations at high pressures and high temperatures has been in the design of the optical cell that can withstand severe conditions, sometimes with corrosive atmosphere. A Raman cell useable under severe conditions has been developed as described elsewhere.[30,31] To obtain the polarized Raman spectra of the totally symmetric N−O stretching of the nitrate ion near 1050 cm^{-1}, we used a TRS-600 triple monochromator with an LN-CCD detector (Princeton Instruments Inc.) cooled at −120 °C and a polarization filter followed by a quartz wedge scrambler between the sample and entrance slit for taking I_{VH} and I_{VV} (V, vertical; H, horizontal) spectra. A 400 mW Coherent (Innova 70) argon ion laser operating at 488 nm was used as the light source. Optical access was given by way of three circular 0° single-crystal sapphire windows, which were sealed to the cell using gold-plated metal foil. A 90° scattering geometry was used, the cell being illuminated from below. The cell was fixed in a stainless steel heating jacket, which was mounted on a translation stage and was finely controlled to the optimum position. The laser beam and optic axis of the sapphire windows were accurately aligned so that our experimental apparatus gave the known depolarization ratio of the 459 and 210 cm^{-1} lines in CCl_4. The scattered light was collected, passed through the polarization filter, and focused into the entrance slit. The I_{VH} and I_{VV} spectra were taken in the range of ±150 cm^{-1} about the band center with a step of 1.10 cm^{-1} at the optical slit widths of 100 μm. Depolarized spectra were accumulated 10 times in the exposure time of 30 s to improve the signal-to-noise ratio. The degree of depolarization ρ(nitrate) was 0.05, in good agreement with the literature value.[11,13]

The sample temperature was determined with a sheathed CA thermocouple at a point of 3 mm from the focal point of the cell. The temperature calibration was validated by measuring the pressure at several temperatures in the liquid−vapor two-phase equilibrium region and comparing the measured temperatures with the known values[7] at the saturation point.[21] The uncertainty was less than 1 °C above 300 °C.[31] After the cell was filled with pure water, the sample solution was very slowly loaded into the already heated and pressurized cell using a conventional high-pressure liquid pump. The sample volume was 0.5 cm^3. The pressure control was achieved by a back-pressure regulator within 0.1 MPa. No decomposition and precipitation of the salt were observed to occur within the pressure and temperature ranges examined.

The spectral signals were collected by a data acquisition system, which was also used for the analog-to-digital conversion (32 bits). The digitized spectral data were used in detailed spectral analyses by a personal computer (DELL OPTIPLEX XMT 5100). The baseline of the spectra was not flat owing to the overlap of the nitrate band and the water liberation band,[14] so a correction for the water liberation by an added salt was made using a fitted function including a polynomial up to 6th order. We attempted to subtract the intensity of the water liberation by making independent measurements in pure water; however, it was not permissible because the intensity in aqueous zinc solution varies with an increase in temperature. The line-shape parameters measured include the proportions of Gaussian and Lorentzian functions, the sum function for the component bands, and the maximum and centroid frequency, and the half-width at half peak height (hwhh) were determined by using a program based on the Levenberg−Marquardt method.[34]

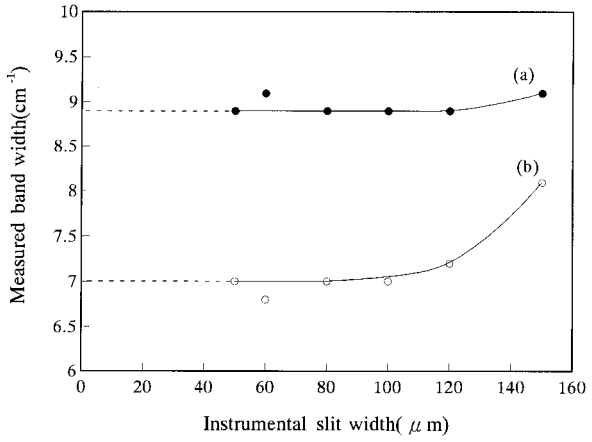

Figure 2. Plot of measured bandwidth against instrumental slit width: (a) I_{VV}; (b) I_{VH}.

Raman Line-Shape Analysis. With $I_{VH}(\omega)$ and $I_{VV}(\omega)$ representing the weak and strong components of the scattered light (ω is the frequency),[35] the baseline correction leads to isotropic and anisotropic profiles:[14]

$$I_{iso}(\omega) = I_{VV}(\omega) - (^4/_3)I_{VH}(\omega) \quad (1)$$

$$I_{aniso}(\omega) = I_{VH}(\omega) \quad (2)$$

$I_{iso}(\omega)$ shows the intrinsic vibrational line shape, and $I_{aniso}(\omega)$ is a convolution of the vibrational line shape and the orientational spectrum. One must separate the two precisely; however, the measured spectrum is a convolution of the true spectrum and the Gaussian slit function $S(\omega)$ such that

$$I'_{iso}(\omega) = \int_{-\infty}^{\infty} I_{iso}(\omega)S(\omega)\, d\omega \quad (3)$$

$$I'_{aniso}(\omega) = \int_{-\infty}^{\infty} I_{or}(\omega)I_{iso}(\omega)S(\omega)\, d\omega \quad (4)$$

where the primed and unprimed functions indicate the measured and true line shapes, respectively. The $I_{or}(\omega)$ denotes the true orientational spectrum. To obtain true line shapes associated with the deconvolution, it is important that the slit function be removed.[36] The effect of slit width coupled with the measured band was determined, and the relationship between the bandwidth for the 1050 cm^{-1} line of the N−O stretch and the instrument slit width is shown in Figure 2. It was thus shown that $I_{VH}(\omega)$ should be determined at a slit with of 100 μm or less to obtain $I_{iso}(\omega)$. $I_{VV}(\omega)$ can be also determined using the same slit setting.

Implicit in the treatment of data is the assumption that $I_{iso}(\omega)$ and $I_{aniso}(\omega)$ are Lorentzian and that vibrational and reorientational profiles are not coupled. The line shape was thus tested for this assumption, and a typical result is shown in Figure 3, in which $I_{aniso}(\omega)$ and $I_{iso}(\omega)$ represent the normalized line shapes of the ν_1 band. A Lorentzian peak is described by the peak intensity $I(\omega)$, the position of peak maximum ω_0, and the hwhh Γ:

$$I(\omega) = I_{max}[1 + ((\omega - \omega_0)/\Gamma)^2]^{-1} \quad (5)$$

The solid line in Figure 3 is calculated according to eq 5 with the observed line widths. $I_{aniso}(\omega)$ and $I_{iso}(\omega)$ are in good agreement with Lorentzian band shapes. $I_{aniso}(\omega)$ is a convolution of $I_{iso}(\omega)$ with $I_{or}(\omega)$, and the $I_{aniso}(\omega)$ is also Lorentzian. $I_{or}(\omega)$ is the component purely due to the observable

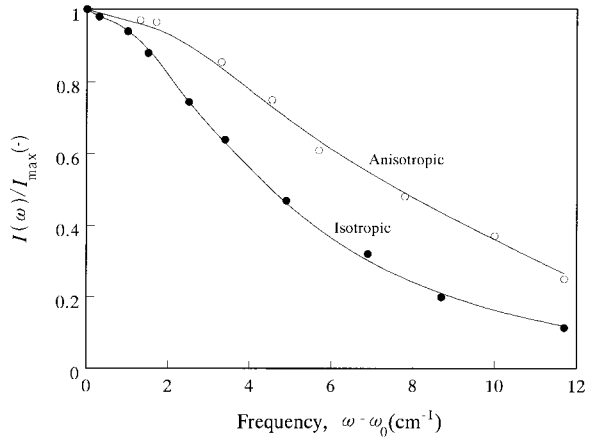

Figure 3. Experimental (circles) and Lorentzian-fitted (lines) isotopic and anisotropic shapes of the ν_1 stretch band for 1.3 M zinc nitrate solution at 20 °C and 30 MPa.

rotation. Thus,

$$\Gamma(\text{aniso}) = \Gamma(\text{iso}) + \Gamma(\text{OR}) \quad (6)$$

where Γ(aniso), Γ(iso), and Γ(OR) denote the Γ values of $I_{aniso}(\omega)$, $I_{iso}(\omega)$, and $I_{or}(\omega)$, respectively. Thus, the Γ(OR) value can be related to the perpendicular orientational relaxation time $\tau_\perp$ as

$$\tau_\perp^{-1} = 2\pi c\Gamma(\text{OR}) \quad (7)$$

where c is the speed of light. Furthermore, the perpendicular diffusion constant $D_\perp$ is given by

$$6D_\perp = \tau_\perp^{-1} \quad (8)$$

Results and Discussion

Identification of Species by Spectral Analysis. Raman spectra of 1.3 M (20 °C and 0.1 MPa) aqueous zinc nitrate solution were measured in the temperature range 20−360 °C at a pressure of 30 MPa. Assignment of the bands of NO_3^- salt solutions has been conducted in detail.[25,26,37−39] Figure 4 shows the Raman spectra of the NO symmetric stretching band (ν_1) centered at 1050 cm^{-1} at 100 and 340 °C. The spectra are fitted well by two components, which indicates that the NO_3^- species form at least two different complexes. Furthermore, the relative area of the lower-frequency band to the higher-frequency band increases with an increase in temperature. As the temperature increases, the dielectric constant significantly decreases,[8] increasing the attractive forces between cations and anions. That is, the observed red shift of the vibration modes results from the strong cation−anion interactions prevailing at higher temperatures and the predominance of neighboring cation−anion pairs that weaken the covalent N−O bond. Therefore, the lower-frequency mode corresponds to the NO_3^- species more strongly associated with the Zn^{2+}, $[Zn(H_2O)_xNO_3]^+$ where $x \leq 6$, and the higher-frequency mode corresponds to the NO_3^- species weakly associated with Zn^{2+} in an environment of water molecules, $Zn^{2+}(H_2O)_6\ NO_3^-$. Such an assignment of the NO stretching modes has been provided elsewhere.[24−26] Hereinafter, the former and the latter are termed the "*bound*" and "*free*" species, respectively, for the sake of convenience. We choose the NO spectra in the ν_1 region instead of that in the ν_4 (deformation mode) region for the above-mentioned analysis because the ν_1 intensity is larger than the ν_4 intensity and the values of the ion-pair constant for the ν_4

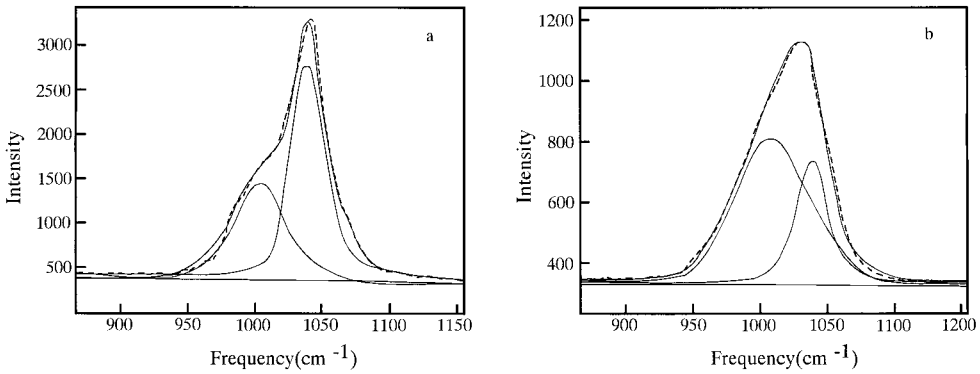

Figure 4. Raman spectra at 100 °C (a) and 340 °C (b). Broken lines are experimental data, and solid lines correspond to deconvoluted curves and their sum.

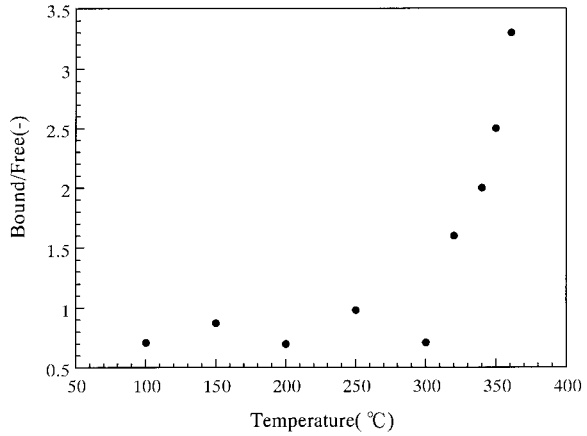

Figure 5. Temperature dependence of intensity ratio of the bound species to the free species in zinc nitrate solution at 30 MPa.

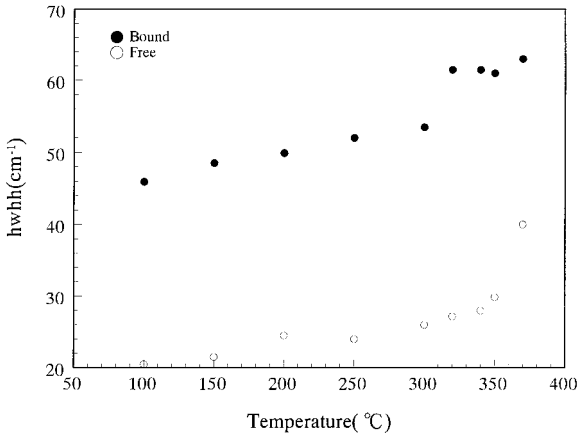

Figure 6. The hwhh of the resolved bands of NO symmetric stretching (ν_1) mode in zinc nitrate solution at 30 MPa.

mode was reported to be remarkably lower than those calculated from the conductivity data.[24,40,41]

Figure 5 shows the temperature dependence of the intensity ratio of the bound species to the free species for the ν_1 mode, on the assumption that the molar scattering coefficient of the NO_3^- is constant under the experimental conditions.[24,26] The ratio of the bound to the free species almost remains unaltered at a value of approximately 0.75 below 300 °C. Above 300 °C the ratio significantly increases and reaches over 3 at 360 °C. Such a break around 300 °C indicates a change in the coordination geometry,[42,43] and the replacement of H_2O molecules in the primary solvation shell of Zn^{2+} by NO_3^- could be promoted at higher temperatures, resulting in enhanced interactions between the Zn^{2+} and NO_3^-. Brill et al. have examined the temperature dependence of the similar relative ratio in a concentrated aqueous zinc nitrate solution (4.50 *m*) in the temperature range 25−450 °C at 29 MPa; however, they observed a monotonic increase of the bound species with increasing temperature.[25,26] In a more concentrated solution, sudden changes in the coordination geometry would not be caused by the temperature change; however, we cannot give a complete explanation at present.

Figure 6 represents the temperature dependence of hwhh of the bound and free species. For each species, the hwhh gradually increases with temperature and above 300 °C it shows a marked increase, suggesting that a change in the coordination geometry occurs around 300 °C. The width of the resolved bands approximately reflects changes in the extent of vibrational relaxation with temperature. The increase in the bandwidth is due to the strong cation−anion interactions prevailing over the N−O vibration motion and leads to faster relaxation. As shown

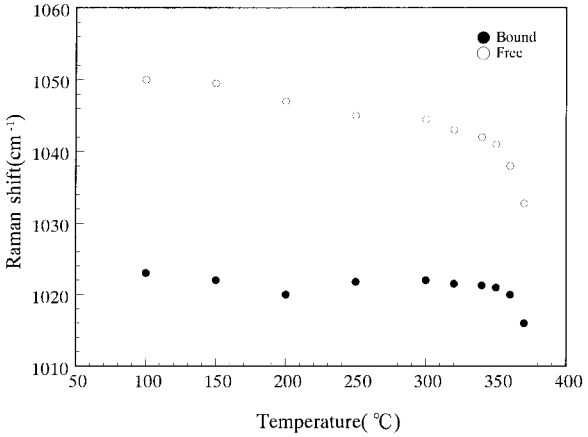

Figure 7. Peak position of the resolved bands from curve fitting of NO symmetric stretching in zinc nitrate solution at 30 MPa.

in Figure 6, the bandwidth of the bound species is larger than that of the free species, indicating that bound species can relax faster than the free species at any temperature examined. We describe the rotational relaxation of the N−O symmetric stretching mode using the Raman line-shape analysis below. Figure 7 shows the temperature dependence of the peak positions (ν_{max}) of the free and bound species. The ν_{max} frequencies of bound and free species almost remain unaltered below 300 °C, but above 300 °C they show a significant decrease. It is probable that a certain change in the coordination geometry takes place above 300 °C. A decrease in the energy of both species means an increase in the cation−anion interaction by the replacement of H_2O molecules about the Zn^{2+}; however, the energy decreases above 300 °C, suggesting that the gradual

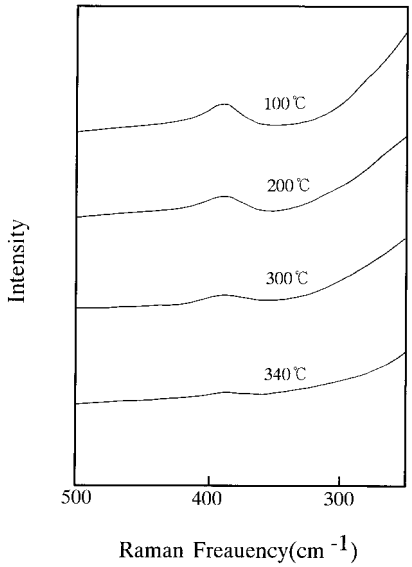

Figure 8. Temperature dependence of the 250−500 cm^{-1} spectral region at 30 MPa.

rearrangement occurs in the bound species in this temperature range, and the direct ion-pair species such as $[Zn\ NO_3]^+$ could be difficult to form.

Hydrolysis of Zn^{2+} ($Zn^{2+} + H_2O = ZnOH^+ + H^+$) in neutral solution facilitates NO_3^- hydrolysis ($NO_3^- + H_2O = HNO_3 + OH^-$) and vice versa. The number of charged species increases with these hydrolysis reactions, and they should become difficult to occur with an increase in temperature owing to a decrease in the dielectric constant of water. Recently, it was shown that water is acidic and can catalyze Beckmann rearrangement of cyclohexanone oxime near the critical point.[44] The evolution of a proton results from the breakdown of the hydrogen-bonding network into dimers and monomers because of large fluctuations of the structure. The hydrolysis of Zn^{2+} and NO_3^- may be suppressed by the acidity of water as well as by the decreasing dielectric constant, corresponding to the increase in the number of bound species with increasing temperature as discussed above.

Estimation of the Number of Water Molecules Bound to Zinc Ion. We observed a band around 390 cm^{-1} in the Raman spectra of 1.3 M aqueous zinc nitrate solution as shown in Figure 8. A band at 386 cm^{-1} at 25 was previously assigned to the symmetric stretching of the haxaaquazinc(II) cation.[24,39] Above 300 °C, the band intensity significantly decreases and the peak position shows a blue shift. These observations reflect the replacement of water molecules about the zinc ion by the nitrate ion. This interpretation is also supported by the changes in the spectra of nitrate ion shown in Figures 5-7.

To explore how change in temperature affects the extent of hydration of the zinc ion, we estimate the average number of water molecules bound to the zinc ion, n_{H_2O}, on the basis of the intensity of the above-mentioned symmetric stretching mode of the haxaaquazinc(II) cation. The n_{H_2O} is defined as

$$n_{H_2O} = 6(I_h/I_{ho}) \quad (9)$$

where I_h is the molar intensity of the aquated zinc ion. We assume that the molar intensity is represented as I_{ho} when all the zinc ion is present as hexaaquazinc(II). In previous stuides[24,37,39] the values of 0.107−0.109 for I_{ho} at 25 °C were reported, and here, we adopt the average value of 0.108. To obtain the molar intensity of the aquated zinc ion, I_h, at each

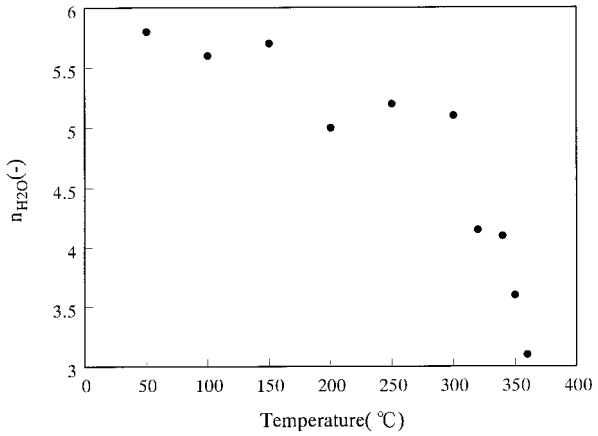

Figure 9. Temperature dependence of average number of water molecules bound to zinc ion at 30 MPa.

temperature, the intensity of the symmetric stretching band of the haxaaquazinc(II) cation measured is divided by the total intensity of the N−O symmetric stretching band at the same temperature.[24] Thus, we can calculate the n_{H_2O} values at the temperatures examined using eq 9. Figure 9 shows the temperature dependence of the n_{H_2O} value. The n_{H_2O} value at 50 °C is 5.8, suggesting the formation of an octahedral configuration around Zn^{2+} at ambient temperature. As the temperature increases, the n_{H_2O} gradually decreases; above 300 °C, however, it decreases sharply to about 3 at 360 °C. This temperature dependence is consistent with those of the ratio of the bound to the free species, hwhh, and Raman peak frequencies as described above. The decrease in the n_{H_2O} above 300 °C clearly indicates the displacement of water molecules from the first solvation shell around zinc ion. Concomitant with the entry of the nitrate ion into the solvation shell is a change in configuration around Zn^{2+} from an octahedral to a tetrahedral configuration like $[Zn(H_2O)_3NO_3]^+$ at 360 °C. Very few data concerning the ion hydration under high pressures and temperatures have been reported so far. Fulton et al. presented the hydration data of strontium and rubidium ions by XAFS measurements.[21,22] The XAFS measurements of the strontium ions in liquid water and supercritical water at 386 °C and 33.9 MPa yielded 7.3 and 3.8 waters of hydration, respectively,[21] while the measurements of rubidium ions in liquid and supercritical water at 424 °C and 38.3 MPa showed 5.6 and 3.4 waters of hydration, respectively.[22] These observations are in agreement with our results of Figure 9.

Rotational Relaxation and $D_\perp$. The $\tau_\perp$ values at temperatures below 340 °C obtained from the hwhh of the pure rotational profile based on eq 7 are shown in Table 1. As the temperature increases, the $\tau_\perp$ decreases from 1.86 ps at 20 °C to 0.25 ps at 340 °C. Using these $\tau_\perp$ values, one can calculate the apparent activation energy for the orientational motion of the NO_3^- species, ΔE_{OR}. The Arrhenius-type plot is shown in Figure 10. The observed temperature dependence is interesting. First, above about 300 °C the rotational relaxation time $\tau_\perp$ decreases significantly. Second, below 300 °C the apparent activation energy ΔE_{OR1} is 2.1 ± 0.3 kcal mol^{-1}, which is about one-half the activation energy of the orientational motion of a water molecule.[45] Above 300 °C, in contrast, a larger activation energy (ΔE_{OR2}) of 6.4 ± 0.1 kcal mol^{-1} is obtained. Last, the temperature dependence displays a major slope break around 300 °C in Figure 10, a trend that is consistent with that of the ratio of the bound species to the free species in Figure 4 and that of the number of n_{H_2O} in Figure 9.

TABLE 1: Orientational Relaxation Time and Rotational Diffusion Constant of the ν_1 Perpendicular Mode of 1.3 M NO_3^- in Water at 30 MPa

temp (°C)	$\tau_\perp$ (ps)	$D_\perp \times 10^{-10}$ [b] (s^{-1})
20[a]	1.77	9.4 (46.3)
20	1.86	9.0 (46.3)
50	1.46	11.4 (48.6)
100	1.25	13.3 (52.2)
150	0.95	17.5 (55.6)
200	0.70	23.9 (58.8)
230	0.62	26.9 (60.7)
250	0.61	27.3 (61.9)
300	0.41	40.7 (64.8)
320	0.33	50.8 (65.9)
340	0.25	66.7 (67.0)

[a] At 0.1 MPa. [b] The values in parentheses represent diffusion constant calculated from SDFR model.

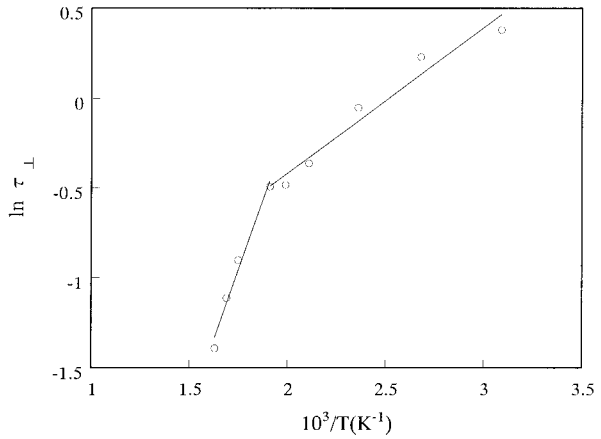

Figure 10. Arrhenius plot of the orientational relaxation time $\tau_\perp$ for 1.3 M NO_3^- in water at 30 MPa. The counterion is Zn^{2+}.

The $\tau_\perp$ values measured are shorter than the lifetime of the surrounding water cage ($>10^{-11}$ s), suggesting that NO_3^- interacts with Zn^{2+} to form a certain solvated species, and as a result, the cation and the anion are significantly closer to each other than predicted by an isotropic distribution. We do not suggest that the $[ZnNO_3]^+$, bearing one unit net charge, always exists as an associated contact ion. The reorientation for the nitrate−zinc ion association must be considerably faster with increasing temperature, especially above 300 °C. In addition, the ΔE_{OR1} value of 2.1 kcal mol^{-1} for the anion is smaller than the activation energy for the orientational motion of a water molecule[45] of 4−5 kcal mol^{-1}. Therefore, it does not seem that the motion of the anion brings about the breakdown of the water−water hydrogen bonds surrounding it at temperatures lower than 300 °C. However, in the temperature range of about 300−340 °C the ΔE_{OR2} value is larger, 6.4 kcal mol^{-1}, and we expect that the reorientating NO_3^- drags the nearest-neighbor water molecules against the remaining water−water network. The zinc ion is strongly coordinated to the NO_3^- at higher temperatures, giving the NO_3^- more vibrational freedom. This explanation has also been supported by the marked increase in the ratio of the bound to the free species in Figure 5 as well as the significant reduction in the number of n_{H_2O} above 300 °C in Figure 9. These results confirm that the dynamics are governed by specific local interactions between NO_3^- species and water.

Experimental values of the rotational diffusion constant $D_\perp$ are shown in Table 1, in which the values of D_i calculated from the slightly damped free rotor (SDFR) model[46−48] are also given. The SDFR model represents a theoretically extreme state and corresponds to molecular reorientation approaching that in the free dilute gas phase where large-angle rotational jumps are assumed and given as[46,47]

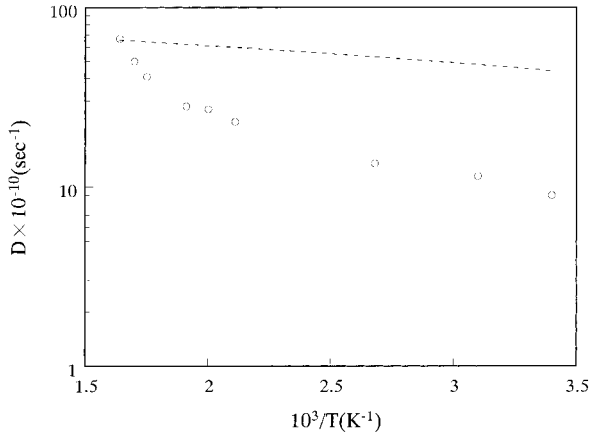

Figure 11. Comparison of experimental values (○) of $D_\perp$ with values of D_i calculated from SDFR theory (- - -).

$$\tau_i = [\pi I_\perp/(12kT)]^{0.5} \quad (10)$$

$$D_i = [kT/(3\pi I_\perp)]^{0.5} \quad (11)$$

where $I_\perp$ is the appropriate moment of inertia of an NO_3^- rotating inertially and k is the Boltzman constant. The $I_\perp$ values are almost independent of nitrate concentration and the kind of cation and are known to be around 20×10^{-39} g cm^2.[11] It was further reported that the $I_\perp$ values do not show an obvious temperature dependence up to 80 °C,[13] and the $I_\perp$ value of 20×10^{-39} g cm^2 is assumed to be applicable to the determination of the diffusion constant in the SDFR model. In Figure 11 the temperature dependence of the experimental $D_\perp$ and the SDFR theoretical D_i values is shown. As shown in this figure, the SDFR model cannot generally describe the reorientation around the perpendicular axis well; however, as the temperature increases, the SDFR theoretical values approach the measured $D_\perp$ at 340 °C and the SDFR theoretical D_i value is in good agreement with the experimental value. One can expect that the intermolecular potential has little dependence on angle[46,47] and that the motion proceeds rapidly around the axis.

Conclusions

Using Raman line-shape analysis, we have made the first direct measurement of the rotational relaxation of the N−O symmetric stretching mode in aqueous zinc nitrate solution at high temperatures up to 340 °C and at a high pressure of 30 MPa. The NO_3^- band profiles were analyzed by asymmetrical curve resolution to obtain the number of species and the optimum line shapes. Such an analysis indicates the formation of two species: one *bound* species where the NO_3^- species is in contact more strongly with the Zn^{2+} and the other *free* species where the NO_3^- species is weakly associated with the Zn^{2+} in an environment of water molecules such as the monovalent cation. Below 300 °C the ratio of the former to the latter remains almost unaltered, but above 300 °C the ratio significantly increases. The increase in bandwidth with temperature is due to the strong cation−anion interactions prevailing over the N−O vibration motion.

The average number of water molecules bound to Zn^{2+}, n_{H_2O}, is estimated using the symmetric stretching mode of the haxaaquazinc(II) cation. As the temperature increases, the n_{H_2O} gradually decreases, but above 300 °C it shows a remarkable

decrease. These results suggest the displacement of water molecules from the first solvation shell around Zn^{2+} and the concomitant entry of NO_3^- into the shell.

For an aqueous solution of zinc nitrate, the perpendicular orientational relaxation time $\tau_\perp$ of the nitrate ion decreases with temperature, being 1.86 ps at 20 °C and 0.25 ps at 340 °C. The reorientation for the nitrate−zinc ion association must be considerably faster with increasing temperature. The SDFR theoretical diffusion constant is in good agreement with the diffusion constant measured at temperatures higher than 300 °C, also suggesting that the motion proceeds rapidly around the axis at the higher temperatures. This explanation has been further supported by the marked increase in the ratio of the bound species to the free species as well as the significant reduction in n_{H_2O} above 300 °C. The apparent activation energy for orientational motion of NO_3^- species up to about 300 °C is 2.1 kcal mol^{-1} and is about one-half the activation energy of the orientational motion of a water molecule in water. Whereas above 300 °C the activation energy increases to 6.4 kcal mol^{-1}. The ΔE value of 2.1 kcal mol^{-1} of the anion is significantly smaller than the activation energy for orientational motion of water, and the motion of the anion does not bring about the breakdown of the water−water hydrogen bonds surrounding it at the lower temperatures. On the other hand, above 300 °C the reorientating NO_3^- drags the nearest-neighbor water molecules against the remaining water−water network.

References and Notes

(1) Thomason, T. B.; Modell, M. *Hazard. Waste* **1984**, *1*, 453.
(2) Barner, H. E.; Huang, C. Y.; T. Johnson, Jacobs, G.; Martch, M. A.; Killilea, W. R. *J. Hazard. Mater.* **1992**, *31*, 1.
(3) Shaw, R. W.; Brill, T. B.; Clifford, A. A.; Eckert, C. A.; Franck, E. U. *Chem. Eng. News* **1991,** *69*, 26.
(4) Li, R.; Savage, P. E.; Szmukler, D. *AIChE J.* **1993**, *39*, 178.
(5) Hatakeda, K.; Ikushima, Y.; Ito, S.; Sato, O.; Saito, N. *Chem. Lett.* **1997**, 245.
(6) Archer, D. G.; Wang, P. *J. Phys. Chem. Ref. Data* **1990**, *19*, 371.
(7) Haar, L.; Gallagher, J. S.; Kell, G. S. *NBC/NRC Steam Tables*; Hemisphere: New York, 1984.
(8) Fermandez, P. R. J.; Corti, H. R.; Japes, M. L. *High-Temperature Aqueous Solutions: Thermodynamic Properties*; CRC Press: Boca Raton, FL, 1992.
(9) Soper, A. K.; Neilson, G. W.; Enderby, J. E.; Howe, R. A. *J. Phys. Chem. Solids* **1977**, *10*, 1793.
(10) Powell, D. H.; Gullidge, P. M. N.; Neilson, G. W. *Mol. Phys.* **1990**, *71*, 1107.
(11) Kato, T.; Umemura, J.; Takenaka, F. *Mol. Phys.* **1978**, *36*, 621.
(12) Kato, T.; Takenaka, F. *Mol. Phys.* **1983**, *46*, 257.
(13) Perrot, M.; Guillaume, F.; Rothschild, W. G. *J. Phys. Chem.* **1983**, *87*, 5193.
(14) Adachi, A.; Kiyoyama, H.; Nakahara, N.; Masuda, Y.; Yamatera, H.; Shimizu, A.; Taniguchi, Y. *J. Chem. Phys.* **1989**, *90*, 392.
(15) Gao, J. *J. Am. Chem. Soc.* **1993**, *115*, 6893.
(16) Gao, J. *J. Phys. Chem.* **1994**, *98*, 6049.
(17) Cui, S. T.; Harris, J. G. *J. Phys. Chem.* **1995**, *99*, 2900.
(18) Cumming, P. T.; Cochran, H. D.; Simonson, J. M.; Mesner, R.; Karaborni, E. *J. Chem. Phys.* **1994**, *94*, 5606.
(19) Balbuena, P. B.; Johnston, K. P.; Rossky, P. J. *J. Phys. Chem.* **1996**, *100*, 2706.
(20) Benning, L. G.; Seward, T. M. *Geochim. Cosmochim. Acta* **1996**, *60*, 1849.
(21) Pfund, D. M.; Darab, J. G.; Fulton, J. L.; Ma, Y. *J. Phys. Chem.* **1994**, *98*, 13102.
(22) Fulton, J. L.; Pfund, D. M.; Wallen, S. L.; Newville, M.; Sten, E. A.; Ma, Y. *J. Chem. Phys.* **1996**, *105*, 2161.
(23) Seward, T. M.; Henderson, C. M. B.; Charnock, J. M.; Dobson, B. R. *Geochim. Cosmochim.* Acta **1996**, *60*, 2273.
(24) Irish, D. E.; Jarv, T. *Appl. Spectrosc.* **1983**, *37*, 50.
(25) Spohn, P. D.; Brill, T. B. *J. Phys. Chem.* **1989**, *93*, 6224.
(26) Spohn, P. D.; Brill, T. B. *Appl. Spectrosc.* **1987**, *41*, 1152.
(27) Ryan, E. T.; Xiang, T.; Johnston, K. P.; Fox, M. A. *J. Phys. Chem.* **1996**, *100*, 9395.
(28) Alia, J. M.; Edwards, H. G. M. *J. Mol. Struct.* **1995**, *354*, 97.
(29) Carpio, R. A.; Mehmed, M.; Yeager, E. *J. Chem. Phys.* **1981**, *74*, 2778.
(30) Ikushima, Y. *Rev. High Pressure. Sci. Technol.* **1997**, *6*, 24.
(31) Ikushima, Y.; Hatakeda, K.; Saito, N.; Arai, M. *J. Chem. Phys.*, in press.
(32) Nafie, L. A.; Peticolas, W. L. *J. Chem. Phys.* **1972**, *57*, 3145.
(33) Amorim Da Costa, A. M. *J. Mol. Struct.* **1978**, *46*, 465.
(34) Marquardt, D. W. *J. Sol. Ind. Appl. Math.* **1963**, *11*, 431.
(35) Colles, M. J.; Griffiths, J. E. *J. Chem. Phys.* **1972**, *56*, 3384.
(36) Bartoli, F. J.; Litovitz, T. A. *J. Chem. Phys.* **1972**, *56*, 404.
(37) Sze, Y.-K.; Irish, D. E. *J. Solution Chem.* **1978**, *7*, 395.
(38) Irish, D. E.; Chang, T. G.; Nelson, D. L. *Inorg. Chem.* **1970**, *9*, 425.
(39) Bulmer, J. T.; Irish, D. E.; Odberg, L. *Can. J. Chem.* **1975**, *53*, 380.
(40) Janz, G. J.; Muller, M. A. *J. Solution Chem.* **1975**, *4*, 285.
(41) Chang, T. G.; Irish, D. E. *J. Solution Chem.* **1974**, *3*, 161.
(42) Carrick, M. T.; James, D. W.; Leong, W. H. *Aust. J. Chem.* **1983**, *36*, 223.
(43) James, D.; Frost, R. L. *Aust. J. Chem.* **1982**, *35*, 1793.
(44) Sato, O.; Ikushima, Y. To be submitted.
(45) Eisenberg, D.; Kauzmann, W. *The Structure and Properties of Water*; Oxford University Press: Oxford, 1969; p 205.
(46) Steele, W. A. *J. Chem. Phys.* **1963**, *38*, 2404.
(47) Steele, W. A. *J. Chem. Phys.* **1963**, *38*, 2410.
(48) Atkins, P. W. *Mol. Phys.* **1969**, *17*, 321.